



Since January 2020 Elsevier has created a COVID-19 resource centre with free information in English and Mandarin on the novel coronavirus COVID-19. The COVID-19 resource centre is hosted on Elsevier Connect, the company's public news and information website.

Elsevier hereby grants permission to make all its COVID-19-related research that is available on the COVID-19 resource centre - including this research content - immediately available in PubMed Central and other publicly funded repositories, such as the WHO COVID database with rights for unrestricted research re-use and analyses in any form or by any means with acknowledgement of the original source. These permissions are granted for free by Elsevier for as long as the COVID-19 resource centre remains active.



Rapid biosensing SARS-CoV-2 antibodies in vaccinated healthy donors

Sumin Bian^{a,1}, Min Shang^{b,1}, Mohamad Sawan^{a,*}

^a CenBRAIN, School of Engineering, Westlake University, China

^b Dept. of Cardiology, Sir Run Run Shaw Hospital, School of Medicine, Zhejiang University, China

ARTICLE INFO

Keywords:

Biosensors
SARS-CoV-2
COVID-19 vaccines
Neutralizing antibodies
Binding antibodies
Biolayer interferometry

ABSTRACT

In this study, we report two fiber optic-biolayer interferometry (FO-BLI)-based biosensors for the rapid detection of SARS-CoV-2 neutralizing antibodies (NAb) and binding antibodies (BAbs) in human serum. The use of signal enhancer 3,3'-diaminobenzidine enabled the detection of NAb, anti-receptor binding domain (anti-RBD) BAbs, and anti-extracellular domain of spike protein (anti-S-ECD) BAbs up to as low as 10 ng/mL in both buffer and 100-fold diluted serum. NAb and BAbs could be detected individually over 7.5 and 13 min, respectively, or simultaneously by prolonging the detection time of the former. The protocol for the detection of BAbs could be utilized for detection of the RBD-N501Y variant with equal sensitivity and speed. Results of the NAb and the anti-RBD BAbs biosensors correlated well with those of the corresponding commercial assay kit. Clinical utility of the two FO-BLI biosensors were further validated using a small cohort of samples randomly taken from 16 enrolled healthy participants who received inactivated vaccines. Two potent serum antibodies were identified, which showed high neutralizing capacities toward RBD and pseudovirus. Overall, the rapid automated biosensors can be used for an individual sample measurement of NAb and BAbs as well as for high-throughput analysis. The findings of this study would be useful in COVID-19 related studies in vaccine trials, research on dynamics of the immune response, and epidemiology studies.

1. Introduction

Recent population-based serosurveys indicated the necessity of national-level vaccination to prevent the resurgence of the coronavirus disease (COVID-19) pandemic, as it is difficult to achieve a herd immunity even within highly exposed COVID-19 communities (Stringhini et al., 2021; He et al., 2021). As COVID-19 vaccines are being rolled out, it is important to address the worldwide problem of scarce vaccine supplies; priorities need to be assigned by taking into consideration the fact that persons who have pre-existing anti-spike IgG antibodies may not need a second dose (Krammer et al., 2021). Testing each person prior to their vaccination will heavily burden the healthcare system in all the countries. A rapid but sensitive serological test that can be easily performed on site and instantly indicate the infection history of an individual, will make this process feasible and subsequently facilitate the development of a more efficient vaccination strategy. Infection history can be confirmed by determining the presence of anti-SARS-CoV-2 IgG-binding antibodies (BAbs) (Liu et al., 2021). Determination of anti-SARS-CoV-2 neutralizing antibodies (NAb) answers questions

regarding COVID-19 vaccine efficacy as well as the dynamics of immune response during infection and post recovery (Wajnberg et al., 2020; Legros et al., 2021). Additionally, the NAb test can aid in screening therapeutic NAb candidates for treating SARS-CoV-2 (Huo et al., 2020; Zhou et al., 2020), and once NAb approved, the NAb test may later serve as a therapeutic drug monitoring tool to optimize efficacy (Papa-michael et al., 2019).

Currently, the majority of BAbs assays used in clinical practice are developed on the basis of ELISA platforms, thereby typically requiring a longer period to obtain results. Lateral flow assays fail to provide quantitative information. Although optics, probes, or microfluidic-based platforms allow a faster readout, the existing methods still require a minimum of half an hour to acquire results (Funari et al., 2020; Swank et al., 2021; Tan et al., 2020; Yang et al., 2021). Graphene-based electrochemical biosensors allow BAbs detection in seconds, but their use in clinical practice awaits proof (Ali Md, et al., 2021; Torrente-Rodríguez et al., 2020). Existing assays for NAb detection include the S-ECD pseudotyped vesicular stomatitis virus assay and vector-based neutralization assay (Nie et al., 2020), both of which require a biosafety level-3

* Corresponding author. 18 Shilongshan Road, Cloud Town, Xihu District, Hangzhou, Zhejiang, 310024, China
E-mail address: sawan@westlake.edu.cn (M. Sawan).

¹ Two first authors contributed equally to the work.

operating environment and the use of cells or real viruses for testing, and a more convenient surrogate virus neutralization test that shows equivalent sensitivity and specificity to the classic NABs assay (Tan et al., 2020). Previously, we developed a surrogate tumor necrosis factor (TNF) neutralization ELISA to conveniently evaluate the neutralization capacities of a batch of monoclonal antibodies against TNF, which yielded similar results as obtained with classic cell-based assays (Bian et al., 2017). Nevertheless, there is a lack of techniques that allow rapid tracking of SARS-CoV-2 BAbS and NABs within approximately 10 min. Such techniques could support on-site detection of a single sample and greatly facilitate vaccine priority management by providing immediate feedback regarding the antibody status of an individual. In addition, the majority of data regarding SARS-CoV-2 antibodies, to date, have been obtained from COVID-19-infected or recovered patients. Real data on how SARS-CoV-2 antibodies exist and evolve in healthy persons who received COVID-19 vaccines, whether mRNA or inactivated, are scarce.

Bilayer interferometry (BLI), which utilizes the thickness on the tip of its optical fiber as a reflection of the number of attached molecules, is a powerful tool for characterizing the interaction between proteins and antibodies (Zhou et al., 2021). The use of BLI for accurate quantification, however, is rare because of its limited signal readout when target concentrations are low in clinical samples. Sufficient signal amplification is required when developing BLI into a biosensor. Gold nanoparticles proved to be an effective enhancer in surface plasmon resonance-based optical biosensors (Bian et al., 2018; Lu et al., 2016), but their enhancing effect in BLI-based optical biosensors seems limited, as reflected by a recent study wherein maximal signals of approximately 3 nm were obtained for semi-quantitative detection of SARS-CoV-2 BAbS (Dzimianski et al., 2020). Meanwhile, 3,3'-diaminobenzidine tetrahydrochloride (DAB), a metal precipitating substrate, combined with secondary antibody-conjugated horseradish peroxidase (HRP), is a more effective strategy for improving BLI signals (Auer et al., 2015; Gandolfini et al., 2017; Gao et al., 2017). The purpose of this study was to develop fiber optic BLI (FO-BLI)-based biosensors for simultaneous and rapid detection of the SARS-CoV-2 IgG BAbS and NABs within approximately 10 min. Furthermore, we aimed to report the profile of both types of antibodies in a group of healthy persons who recently received local COVID-19 inactivated vaccines.

2. Materials and methods

2.1. Materials and agents

The biotinylated SARS-CoV-2 spike RBD-His recombinant protein, SARS-CoV-2 spike RBD(N501Y)-His recombinant protein, SARS-CoV-2 spike ECD (S1+S2)-His recombinant protein, SARS-CoV-2 spike pseudovirus (containing 10^{10} virus copies/mL and 860 ng/mL of SARS-CoV-2-S1), human recombinant ACE2 protein (biotinylated), rabbit SARS-CoV-2 spike neutralizing antibody, SARS-CoV-2 spike RBD recombinant protein (HRP labeled, customized), SARS-CoV-2 (2019-nCoV) Spike RBD Antibody Titer Assay Kit, and SARS-CoV-2 (2019-nCoV) Inhibitor Screening ELISA Kit were purchased from Sino Biologicals (Beijing, China). The anti-SARS-CoV-2(S1)-6 monoclonal antibody (S309) (referred to as MA-RBD S309, Cat ATMA10183M0) was purchased from AtaGenix (Wuhan, China). The SARS-CoV-2 RBD aptamer sequences (CoV-2-RBD-1C: CAGCACCGACCTGTGCTTTG GGAGTGCTGTC-CAAGGGCGTTAATGGACA; CoV-2-RBD-4C: ATCCAGAGTGACG CAG-CATTTTCATCGGGTCCAAAAGGGGCTGCTCGGGATTGCGGATATGGACG) reported by Song et al. (2020), were used for designing primers, which were synthesized by Sangon Biotech (Shanghai, China). Single donor human serum off the clot and human full blood (Innovative Research, Shanghai, China), biotinylating kit (Genomere, Cat G-MM-IGT, Suzhou, China), HRP conjugation kit and rabbit anti-human IgG H&L (HRP) (Abcam, Shanghai, China); 3,3'-diaminobenzidine (DAB) enhanced liquid substrate system tetrahydrochloride, bovine serum albumin (BSA), and Tween 20 (Sigma-Aldrich, Shanghai, China); Zeba™ Spin Desalting

Ccolumns, 7K MWCO, 0.5 mL), and Pierce™ BCA Protein Assay (Cat 23227) (Thermo Scientific, Shanghai, China) were purchased from the indicated suppliers. 96-well polystyrene black microplates were obtained from Greiner Bio-One GmbH (Shanghai, China). Freshly prepared phosphate-buffered saline (PBS, 10 mM, pH 7.4) containing 0.02% Tween20 and 0.1% BSA (referred to as PBS-T-BSA) was used throughout this work for all steps unless otherwise specified. The Octet® K2 2-Channel System, along with streptavidin sensors from Sartorius Group (Gottingen, Germany), was used to conduct all optical measurements in this study. A Biotek ELx808 absorbance microplate reader (BioTek Instruments, USA) was used for ELISA measurements to read the optical density (OD) values.

2.2. Synthesis of proteins for use in streptavidin sensors

Based on the more stable signals obtained from biotinylated antigens on streptavidin sensors over time than from His-labeled antigens on anti-penta-His HIS1K biosensors (Dzimianski et al., 2020), streptavidin sensors were used throughout this study. Three types of antigens, SARS-CoV-2 extracellular domain of spike protein (S-ECD), receptor binding domain (RBD), and RBD-N501Y mutation, were labeled with biotin for interaction. Biotinylation of S-ECD and RBD-N501Y was conducted according to the biotinylating kit protocol, followed by a desalting protocol to remove any unbound biotin, and a BCA protein assay protocol. Biotinylated RBD was commercially ordered and resuspended in PBS-T buffer. Biotinylated proteins were stored at 4 °C until further use.

2.3. Establishing FO-BLI biosensors for SARS-CoV-2 BAbS detection in buffer and serum

Optical fibers used in this study are transparent and made of glass, allowing the transmission of white light inside. The total length of fibers is measured to be approximately 2.74 cm, consisting of 1.30 cm of fibers and 1.44 cm of fiber holder and robot arm connector (to allow automated operation controlled by the system). The fibers tip contains two layers: the optical titanium oxidation layer and the biocompatible aminosilane layer, both in nanometer in length. The aminosilane layer can be further modified with various functional groups such as streptavidin to allow the specific binding with biotinylated molecules (Fig. 1A).

Streptavidin fibers, alternatively being named as streptavidin sensors, were used throughout this study. Fibers functionalized with biotinylated RBD were used to capture RBD-specific BAbS (*i.e.*, anti-RBD BAbS) in a sandwich binding format (Fig. 1B). MA-RBD S309, a recombinant human IgG1 antibody against RBD but slightly cross-reacting with SARS-CoV-1, was used as the BAbS assay calibrator. Detection was performed using HRP-conjugated secondary antibody rabbit anti-human IgG H&L (r-anti-human IgG-HRP), followed by signal amplification via DAB, the metal chelator. RBD-specific BAbS detection was performed in two different sample matrices: (i) PBS-T-BSA buffer with MA-RBD S309 spiked from 0 to 500 ng/mL: 0–10 – 50–100–500 ng/mL, and (ii) 100-fold diluted serum spiked with MA-RBD S309 spiked from 0 to 500 ng/mL: 0–10 – 50–100–500 ng/mL. Serum was diluted in PBS-T-BSA buffer. The washing process was performed between each step to remove unbound materials. All FO-BLI measurements were conducted at 30 °C with shaking at 1000 rpm.

The process for establishing the S-ECD-specific BAbS (*i.e.*, anti-S-ECD BAbS) and RBD-N501Y-specific BAb (*i.e.*, anti-RBD N501Y BAbS) biosensors is the same as that described above (Fig. 1B). For the three BAb biosensors, biotinylated proteins were diluted to 1 µg/mL in corresponding buffers and the capture antigen shifts were controlled to reach approximately 0.5 nm to avoid potential steric hindrance when capturing antibodies in the samples. The signals delivered from the enhancer DAB were proportional to the amount of r-anti-human IgG-HRP in the underlying complex.

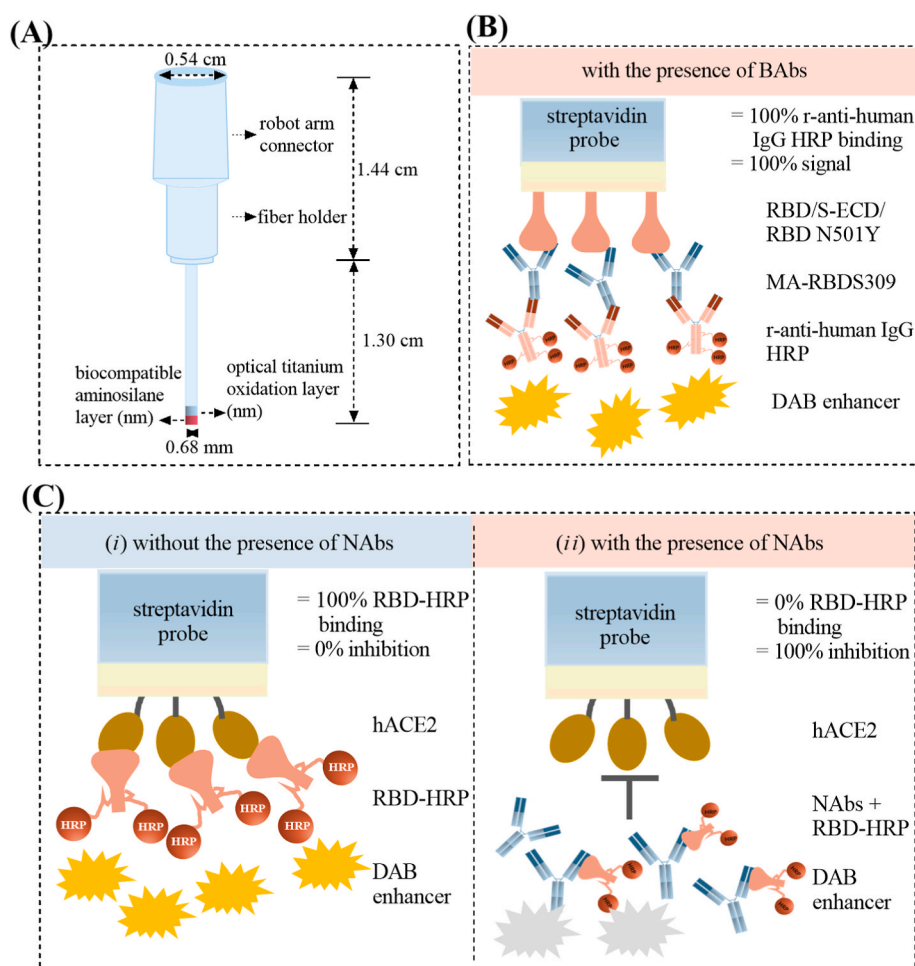


Fig. 1. The optical fiber structure and the general principles of optical biosensors for SARS-CoV-2 antibody detection on the fiber. (A) The three-dimensional structure, parameters, and materials of the optical fibers. (B) Principle of the FO-BLI biosensor for rapid detection of BAbs via a sandwich binding format. The BAbs are specific towards RBD, full length protein S-ECD and RBD mutation N501Y. (C) Principle of the FO-BLI biosensor for rapid detection of NAbs via a competitive binding format. In this bioassay, (i) when no NAbs exist, the binding between RBD-HRP and hACE2 contributes to high detection signals, while (ii) the presence of NAbs blocks HRP-conjugated RBD from binding to immobilized hACE2 protein. In both bioassays, DAB significantly amplified the optical signals.

2.4. Establishing FO-BLI biosensors for SARS-CoV-2 NAbs detection in buffer and serum

Sensors functionalized with biotinylated human ACE2 (hACE2) were used to capture SARS-CoV-2 NAbs in a competitive binding format (Fig. 1C). A rabbit SARS-CoV-2 spike neutralizing antibody against RBD (r-NAb-RBD), which is highly specific and has an affinity of 0.006 nM for SARS-CoV-2 RBD, was utilized as the NAbs assay calibrator. The assay used HRP-conjugated RBD (RBD-HRP) and DAB for competition and detection and for signal amplification, respectively. As shown in Fig. 1C, when no or a limited amount of NAbs was present in a sample, the binding of RBD-HRP to immobilized hACE2 proceeded smoothly and sufficient signals were obtained. When high amounts of high-affinity NAbs are present, RBD-HRP binds specifically with NAbs and therefore can fail to bind immobilized hACE2, resulting in very weak signals. For the NAbs biosensor, 5 $\mu\text{g}/\text{mL}$ of biotinylated hACE2 in PBS-T buffer was used to reach approximately 1.0 nm of loading shifts for sufficient binding. NAbs were detected in the same two matrices as those for anti-RBD BAbs: (i) PBS-T-BSA buffer with r-NAb-RBD spiked from 0 to 500 ng/mL: 0–10–50–100–500 ng/mL and (ii) 100-fold diluted serum with r-NAb-RBD spiked from 0 to 500 ng/mL: 0–10–50–100–500 ng/mL. Spiked samples were mixed with RBD-HRP in equal volumes prior to testing. As described in section 2.3, washing was carried out in between steps, and the generated signals were proportional to the amount of RBD-HRP in the underlying complex. The shifts of the negative control at 0 ng/mL were used as the reference, and the inhibition per point per sample was calculated as shown in Eq. (1).

$$\text{Inhibition} = \left(1 - \left(\frac{\text{shift value of sample}}{\text{shift value of negative control}} \right) \right) \times 100 \quad (1)$$

2.5. Assay limits and cut-off values

The assay values for the limit of detection (LOD), limit of quantification (LOQ), cut-off for detection (Cut-off D), and cut-off for quantification (Cut-off Q) were calculated as described in our previous study (Bian et al., 2017). The control serum samples were obtained from four healthy volunteers with no vaccine injection, no coronavirus infection, and no presence of anti-S-ECD IgG antibodies. An assay dilution factor of 100-fold was used to transfer the calculated LOD and LOQ to Cut-off D and Cut-off Q, respectively.

2.6. Pre-clinical validation of the developed FO-BLI NAbs biosensor

The developed NAbs biosensor was preliminarily evaluated using three monoclonal antibodies (the NAbs calibrator r-NAb-RBD, the BAbs calibrator MA-RBD S309, one monoclonal antibody targeting SARS-CoV-2 S2 (MA-S2)), and two literature-reported SARS-CoV-2 RBD aptamers (CoV-2-RBD-1C and CoV-2-RBD-4C) spiked in pure buffer. In brief, serial concentrations of r-NAb-RBD (0–20 nM), MA-S309 (0–1000 nM), MA-S2 (0–333.3 nM), CoV-2-RBD-1C (0–1000 nM), and CoV-2-RBD-4C (0–1000 nM) were added to the RBD-HRP solution in a 1:1 vol ratio. The inhibition of each sample at each concentration point (a total of 6–8 points per sample) was measured using the FO-BLI NAbs biosensor and compared in parallel with the data obtained from a commercial SARS-CoV-2 Inhibitor Screening ELISA Kit. The ELISA took

2.5 h to complete and OD values were read using an in-house ELISA reader. The OD of the negative control at 0 ng/mL was used as the reference, and the inhibition per point per sample was calculated as shown in Eq. (2).

$$\text{Inhibition} = \left(1 - \left(\frac{\text{OD value of sample}}{\text{OD value of negative control}} \right) \right) \times 100 \quad (2)$$

2.7. Clinical validation using a batch of human serum samples

To evaluate the clinical utility of the established BAbS and NAbS bioassays, 16 healthy adult volunteers (aged 18–60 years) who recently received inactivated vaccines (CoronaVac Sinovac Biotech or BBIBP-CorV Sinopharm), preferably two doses, were enrolled. This study was approved by the Institutional Review Board of Westlake University (20210301BSM001) and the Sir Run Run Shaw Hospital, School of Medicine Zhejiang University (research 20210706-7). Informed consent was obtained from all the participants. Samples were collected at a random time point after day 7 post-injection per individual, to ensure a sufficient time window for antibody production, and de-identified afterwards. The status of anti-RBD BAbS in these samples was first evaluated using a commercial SARS-CoV-2 RBD antibody titer assay under a 100-fold dilution. All samples were analyzed in duplicate using the in-house established Anti-RBD BAb, Anti-S-ECD BAbS and SARS-CoV-2 NAbS biosensors, to systematically profile the status of specific IgG antibodies in each sample. BAbS concentrations for both anti-RBD and anti-S-ECD were defined as $\mu\text{g/mL}$ of MA-RBD S309 equivalents, and NAb concentrations were expressed as $\mu\text{g/mL}$ of r-NAb-RBD equivalents.

2.8. Evaluation of the effects of spike protein and pseudovirus on high-quality serum NAbS

The neutralization capacity of the identified high-quality NAb-positive samples was further confirmed using a series of RBD and pseudovirus concentrations. Briefly, NAb-positive samples were mixed with increasing concentrations of S-ECD (0–4–10–20 $\mu\text{g/mL}$) and pseudovirus (10-fold and 0-fold diluted) in equal volumes, followed by 30 min preincubation at 24 °C on a shaker at 450 rpm. Following appropriate dilution, residual binding of the NAbS mixture was detected using the NAbS assay.

2.9. Statistics

To quantify the correlation and agreement of inhibition of SARS-CoV-2 NAbS in three antibodies and two aptamers obtained from a commercial ELISA kit and the developed NAbS biosensor, GraphPad Prism 9.02 (GraphPad Software, California, USA) was used to determine the Pearson r correlation coefficient and SPSS Statistics v.26 (IBM, New York, USA) was used to calculate the intra-class correlation coefficient (ICC). For calculating the ICC, the “two-way mixed single measure test (absolute agreement)” was applied. Difference between the antibody-positive and antibody-negative samples was analyzed using the two-tailed t -test of GraphPad Prism. Inhibition curves for the FO-BLI NAbS biosensor and the half maximal inhibitory concentration (IC50) were measured using “dose-response-inhibitor: log (inhibitor) vs normalized response,” while binding curves were for the FO-BLI BAbS biosensors were assessed using “one-site: specific binding” in nonlinear regression. Results with a P -value less than 0.05 were considered statistically significant.

3. Results

3.1. FO-BLI biosensors for detection of SARS-CoV-2-specific BAbS towards RBD, S-ECD, and RBD-N501Y in 100-fold diluted serum

The assay conditions of the FO-BLI biosensors for the detection of

SARS-CoV-2-specific BAbS towards S-ECD, RBD, and RBD-N501Y, respectively, in both buffer and serum, are summarized in Table 1, with the principles elaborated in Fig. 1B. For the BAb biosensors, the total detection time was 13 min, including 5 min for capture, 5 min for detection, 2 min for signal amplification, and 30 s for two washings in between. Pre-coating of biotinylated proteins onto the sensor surfaces took 30–70 s, followed by 30 s of washing. Control of nonspecific binding from the matrix was achieved through a 100-fold sample dilution and the addition of the blocking agents Tween 20 and BSA in the buffer. Desirable specific binding of BAbS was achieved by balancing the levels of HRP-labeled detection antibodies with the levels of DAB enhancer, as the levels of both are typically related to its concentration and incubation time. High concentrations of both parameters often resulted in a fast rise in the signal to 40–50 nm (Fig. 2A) and caused sensors to fail due to overloading of the tips. To avoid overloading and for consistent signal generation, concentrations of the detection antibodies were adjusted step-by-step for each bioassay; additionally, a 200-fold dilution of DAB into its substrate buffer, combined with 2 min of incubation, was adopted in all developed bioassays. The shifts at the highest concentration points were controlled at 15 nm. One representative binding profile of MA-RBD S309 in buffer with RBD as the capture antigen achieved via the enhancer is shown in Fig. 2B. Using these defined parameters, calibration curves for specific anti-RBD, anti-ECD, and anti-RBD N501Y BAbS were generated by spiking a series of concentrations of MA-RBD S309 ranging from 0 to 500 ng/mL into 100-fold serum (Fig. 2C).

3.2. FO-BLI biosensor for detection of SARS-CoV-2 NAbS in 100-fold diluted serum

The assay conditions of the FO-BLI biosensors for the detection of SARS-CoV-2-specific NAbS in both buffer and serum are summarized in Table 1, with the corresponding principles elaborated in Fig. 1C. For the NAb biosensors, the total detection time was 7.5 min, including 5 min for both capture and detection in the mixture of samples and RBD-HRP, 2 min for signal amplification, and 30 s for washing. Coating of biotinylated hACE2 to the sensor tips typically took 30–70 s, followed by 30 s of washing. Control of nonspecific binding and sufficient specific binding was achieved as described above for the FO-BLI BAbS biosensors. One representative binding profile of r-NAb-RBD in buffer with hACE2 as the capture antigen achieved via the enhancer, is shown in Fig. 2D.

Calibration curves for specific NAbS detection were generated by spiking a series of concentrations of r-NAb-RBD ranging from 0 to 5000 ng/mL in buffer and 100-fold serum (Fig. 2E). Specifically, a linear regression calibration curve was generated ($Y = 0.301 * X + 0.793$, $R^2 = 0.992$) when r-NAb-RBD concentration ranged from 0 to 250 ng/mL in the diluted serum (inset, Fig. 2E), which could be used for further validation of clinical samples.

3.3. Pre-clinical validation of the developed FO-BLI NAbS biosensor

The inhibition data of three SARS-CoV-2 antibodies and two SARS-CoV-2 aptamers obtained from the developed FO-BLI NAb biosensor were similar to those obtained from a commercial inhibitor screening ELISA kit (Fig. 3A–E). A comparison between the inhibition values measured using the FO-BLI NAbS biosensor versus the ELISA kit revealed a Pearson’s correlation of 0.859 ($p < 0.0001$) and an ICC coefficient of 0.847 ($p < 0.0001$; Fig. 3F).

3.4. Quantification of anti-RBD BAbS, anti-S-ECD BAbS and anti-SARS-CoV-2 NAbS in sera from vaccine-injected healthy donors

The baseline characteristics of the enrolled 16 vaccinated healthy donors (referred to as V-HD) are described in Table 2 (62.5% female, mean age of 27.9 y [STD: 2.7]). Except for V-HD7 and V-HD16 donors

Table 1

Assay conditions of the established FO-BLI biosensors for both SARS-CoV-2 BAbs and SARS-CoV-2 NAbs rapid detection in buffer and serum.

Assay conditions*		Anti-RBD BAbs	Anti-S-ECD BAbs	Anti-RBD N501Y BAbs	NAbs
Immobilize Protein	Probes	Streptavidin sensor	Streptavidin sensor	Streptavidin sensor	Streptavidin sensor
	Capture protein	Biotinylated RBD	Biotinylated S-ECD	Biotinylated RBD-N501Y	Biotinylated hACE2
Target Capture	Capture protein shift	0.55 ± 0.03 nm (n = 12)	0.55 ± 0.01 nm (n = 12)	0.51 ± 0.03 nm (n = 12)	1.10 ± 0.03 nm (n = 12)
	Loading time	30–70 s	30–70 s	30–70 s	30–70 s
	Sample matrix	Buffer, serum	Buffer, serum	Buffer, serum	Buffer, serum
	Sample dilution	1/100	1/100	1/100	1/100
Target Detection	Incubation time	5 min	5 min	5 min	5 min
	Detection antibody or protein	Rabbit anti-human IgG-HRP	Rabbit anti-human IgG-HRP	Rabbit anti-human IgG-HRP	RBD-HRP
	Detection agent conc.	1/20.000	1/1.000	1/10.000	1/1.000
Signal Amplification	Detection time	5 min	5 min	5 min	done with target capture; 30 s in buffer instead
	Signal enhancer	DAB	DAB	DAB	DAB
	Enhancer conc.	1/200	1/200	1/200	1/200
Assay Properties	Enhancing time	2 min	2 min	2 min	2 min
	Assay calibrator	MA-RBD S309	MA-RBD S309	MA-RBD S309	r-NAb-RBD
	Detection range	10–500 ng/mL	10–500 ng/mL	10–500 ng/mL	10–5000 ng/mL
	Cut-off D	0.47 µg/mL	0.40 µg/mL	Not studied	0.36 µg/mL
	Cut-off Q	1.0 µg/mL	1.0 µg/mL	Not studied	0.5 µg/mL
	Sample volume	5 µL	5 µL	5 µL	5 µL
	Sample-to- result time	13 min	13 min	13 min	7.5 min
	Operation	Partial automatic	Partial automatic	Partial automatic	Partial automatic
	Reprodu-cible across labs	Yes	Yes	Yes	Yes

Note: *a 30 s washing step was included in between steps for all the FO-BLI biosensors.

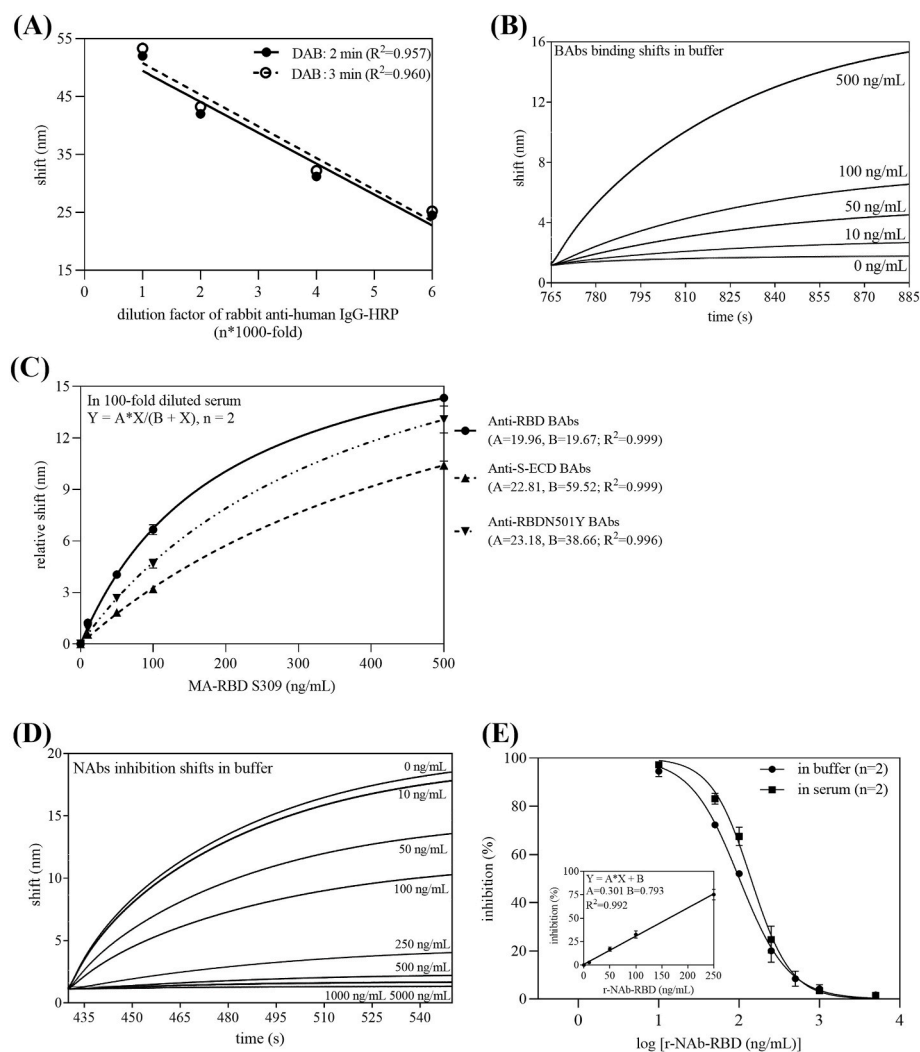


Fig. 2. (A) The binding strength trends obtained when the secondary antibody-HRP conjugate, in a series of dilutions from 1000- to 6000-fold, reacts with DAB enhancer for 2 min and 3 min, respectively. (B) Representative non-linear binding profiles of the Anti-RBD BAbs biosensor after signal enhancement, with the assay calibrator MA-RBD S309 ranged from 0 to 500 ng/mL in buffer. (C) Standard binding curves of the FO-BLI biosensors for anti-RBD BAbs, anti-S-ECD and anti-RBD N501Y in 100-fold diluted serum, respectively. (D) Representative non-linear inhibition profiles of the SARS-CoV-2 NAbs biosensor after signal enhancement, with the assay calibrator r-NAb-RBD ranged from 0 to 5000 ng/mL in buffer. (E) Standard inhibition curves of the SARS-CoV-2 NAbs biosensor in buffer and 100-fold diluted sera, with the assay calibrator r-NAb-RBD ranged from 10 to 5000 ng/mL. A range of 10–250 ng/mL r-NAb-RBD in spiked sera produced a linear-regression calibration curve (inserted). Each sample was measured in duplicate.

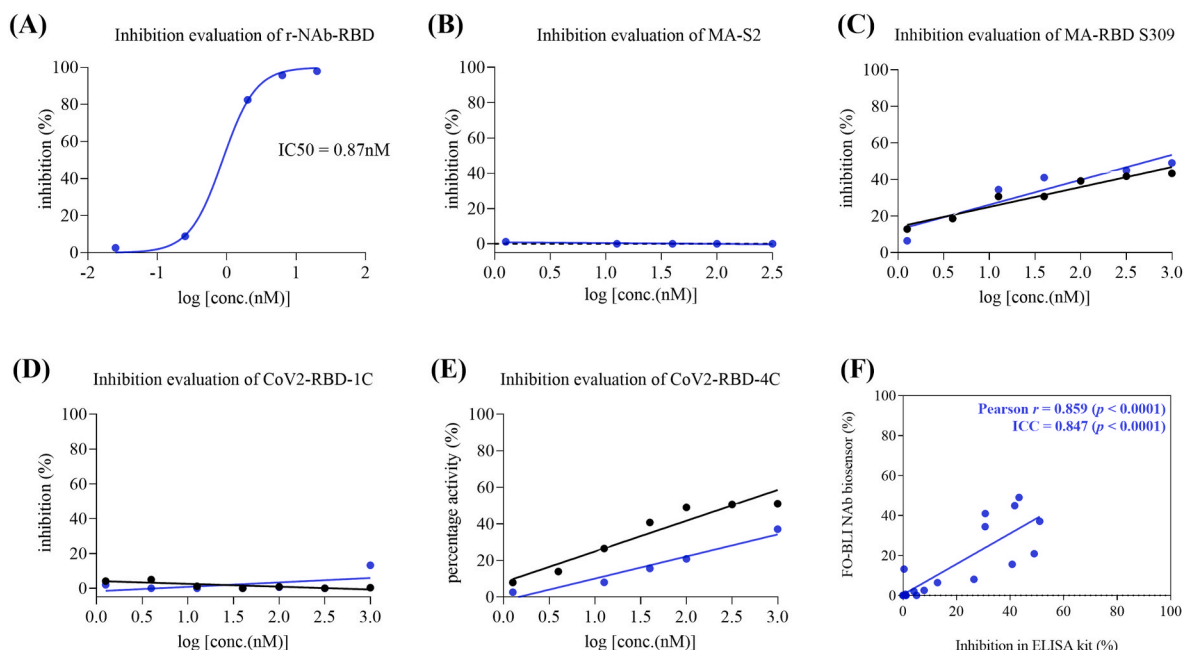


Fig. 3. Inhibition of three monoclonal antibodies and two aptamers against SARS-CoV-2 RBD as measured using both the FO-BLI NAb biosensor (blue lines) and a commercial inhibitor screening ELISA kit (black lines). (A) The NAb assay calibrator r-NAb-RBD was determined to have an IC₅₀ of 0.87 nM, close to the IC₅₀ of 0.59 nM measured by the kit as reported in the product's official document. (B) Inhibition of MA-S2, a non-neutralizing antibody against S2; dashed line indicates a theoretical 0% neutralizing capacity. (C) Inhibition of MA-RBD S309, the SARS-CoV-2 Bab biosensors calibrator; both assays revealed limited inhibition for this antibody. (D) Inhibition of the literature-reported RBD-specific aptamer CoV-2-RBD-1C; both assays reported non-neutralization for it. (E) Inhibition of the literature-reported RBD-specific aptamer CoV-2-RBD-4C; both assays reported limited neutralization for it. (F) Correlation and agreement between inhibition values obtained from both methods; data generally aligned with each other.

Table 2

Baseline characteristics of the 16 participants who received inactivated vaccines with no history of coronavirus infection.

Healthy donors	Gender	Age	First or second dose	Number of days post vaccine injection
V-HD1	Female	26	Second dose	128
V-HD2	Female	31	Second dose	19
V-HD3	Male	26	Second dose	146
V-HD4	Male	30	Second dose	53
V-HD5	Male	33	Second dose	44
V-HD6	Female	27	Second dose	44
V-HD7	Female	26	First dose	13
V-HD8	Male	26	Second dose	85
V-HD9	Female	25	Second dose	30: sample of V-HD9 59: sample of V-HD9-2
V-HD10	Female	27	Second dose	120
V-HD11	Female	31	Second dose	44
V-HD12	Male	27	Second dose	20
V-HD13	Female	24	Second dose	47
V-HD14	Male	28	Second dose	66
V-HD15	Female	32	Second dose	175
V-HD16	Female	28	First dose	14

who only received the first doses when enrolled, all serum samples (one sample sampled per donor) were collected following the second dose, with a mean post-day sampling of 72 (STD: 48.2).

The prevalence of anti-RBD IgG BAbs in individual serum samples was first analyzed using an RBD antibody titer assay kit. As determined from four healthy control serum samples, the assay had a cut-off OD value of 0.19 at a 100 × dilution (dashed line, Fig. 4A), and samples with OD < 0.19 (V-HD7) were deemed as negative. Using this kit, 15 out of 16 V-HD samples were identified as anti-RBD antibody-positive samples (Fig. 4A). All samples were analyzed in duplicate. Of note, the V-HD3 sample with a signal intensity close to the cut-off OD was determined as negative in the first measurement, but positive in the following two

measurements (0.25 ± 0.06 , $n = 3$).

All 16 V-HD samples were further analyzed using the developed Anti-RBD BAB, Anti-S-ECD BAB, and most importantly, the Anti-SARS-CoV-2 NAb biosensors. Regarding the Anti-RBD BAB measurements, results of all samples, but V-HD3, agreed with those obtained from the above-mentioned ELISA kit, that is, 14 out of 16 were anti-RBD positive (87.5%, Fig. 4Bi, left) at the time point sampled. V-HD3 was reported to be negative in the Anti-RBD BAB biosensor, and this negativity was confirmed from the measurement obtained using the anti-S-ECD BAB biosensor. As shown in Fig. 4Bi (left), the levels of anti-RBD antibodies produced inside the body following vaccine injection varied significantly ($0.63\text{--}14.0 \mu\text{g/mL}$ equivalent) among individuals. The difference between the positive and negative samples was statistically significant ($P = 0.01$) in the two-tailed *t*-test (Fig. 4Bi, right). Regarding measurements of the anti-S-ECD BAbs, all antibody-positive samples identified as mentioned above showed anti-S-ECD positivity (14 out of 16 donors; 87.5%) with overall much higher concentrations reported (ranged from 1.01 to 38.02 $\mu\text{g/mL}$ equivalent; Fig. 4Bii, left). The difference between the positive and negative samples remained statistically significant ($P = 0.004$; Fig. 4Bii, right).

Regarding NAb measurements, at the time point when samples were randomly taken, 6 of the 16 V-HD were identified as SARS-CoV-2 NAb-positive (37.5%; Fig. 4Biii, left). One sample showed an NAb level of 0.5 $\mu\text{g/mL}$ equivalent and the remaining 5 samples showed NAb concentrations between 1.07 and 3.84 $\mu\text{g/mL}$ equivalents, indicating effective NAb production in these volunteers to protect from coronavirus attack. A remarkable difference between the NAb-positive and-negative samples was observed ($P < 0.0001$; Fig. 4Biii, right).

Among all the donated samples, the V-HD9 sample reported the maximal signal intensities in the four types of measurements (Fig. 4A and B). The particularly high levels of anti-S-ECD and anti-RBD antibodies and the relatively high levels of NAb in this sample demonstrated that V-HD9 is a high-quality antibody producer. For research purposes, one extra sample, referred to as V-HD9-2, collected 29 days

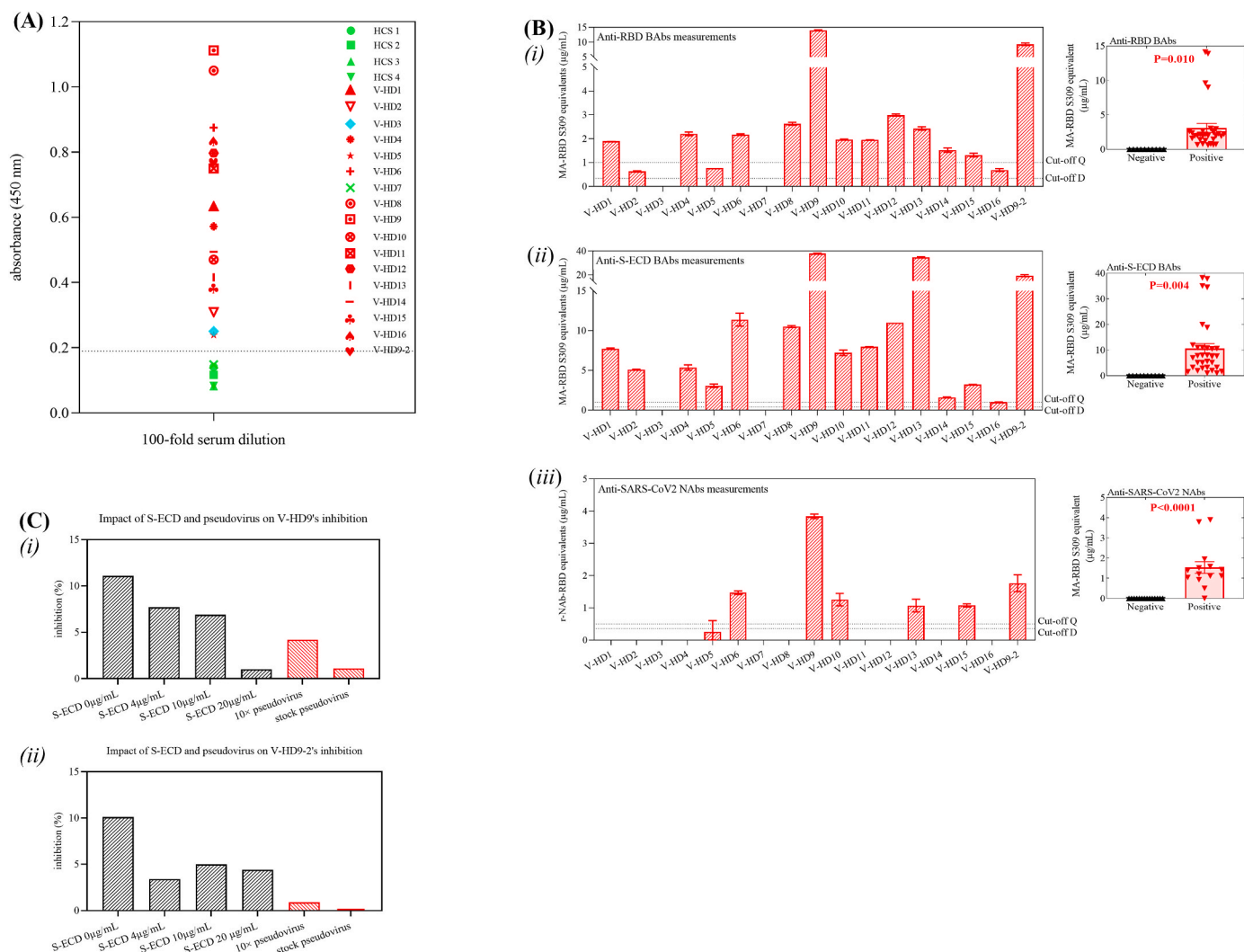


Fig. 4. Detection of anti-RBD, anti-S-ECD BAbs and anti-SARS-CoV-2 NAbs in sera of 16 individual vaccine-injected healthy donors (V-HD1 to V-HD16; V-HD9-2 is the second sample from V-HD9). (A) Prevalence of the anti-RBD antibodies in the 16 donors measured using a commercial RBD antibody titer assay kit. Dashed line indicates the kit's cut-off for detection at 0.19 in absorbance. (Bi) Measurements of anti-RBD antibodies in the 16 donors using the Anti-RBD BAB biosensor. Statistical comparison between the anti-RBD BAB positive and negative samples is listed on the right side. (Bii) Measurements of anti-S-ECD antibodies in the 16 donors using the Anti-S-ECD BAB biosensor. Statistical comparison between the anti-S-ECD BAB positive and negative samples is listed on the right side. (Biii) Measurements of anti-SARS-CoV-2 NAbs in the 16 donors using the Anti-SARS-CoV-2 NAb biosensor. Statistical comparison between the NAbs positive and negative samples is listed on the right side. Dashed lines represent the Cut-off D (Cut-off for Detection) and Cut-off Q (Cut-off for Quantification) of the corresponding assay, all listed in Table 1. Error bars were from duplicate measurements. (C) Inhibition of hACE2–RBD binding by the two screened high-quality NAb serum antibodies: (i) sample of V-HD9 and (ii) sample of V-HD9-2. Inhibition was calculated in the presence of increasing concentrations of S-ECD (0, 4, 10 and 20 µg/mL) and spike pseudovirus (10 × and stock) and assessed using the SARS-CoV-2 NAb biosensor (n = 1).

after the first sample, was requested from this participant and found to contain high levels of anti-S-ECD and anti-RBD antibodies as well as high levels of NAb.

3.5. Evaluation of the effect of spike protein and pseudovirus on the high-titer NAb samples

Under a 100 × sample dilution, the neutralizing capacities of the two identified high-titer NAb samples, V-HD9 (Fig. 4Ci) and V-HD9-2 (Fig. 4Cii), decreased gradually with increasing concentrations of spike protein and spike pseudovirus. When spiked with 20 µg/mL of S-ECD and stock pseudovirus (containing 10¹⁰ virus copies/mL and 860 ng/mL of SARS-CoV-2 S1), the V-HD9 sample completely lost its inhibitory effect on RBD (inhibition of 1.0% and 1.1%, respectively). The V-HD9-2 sample fully lost its inhibition of RBD when spiked with 10 × stock pseudovirus, with inhibition of 0.9% and 0%. These data indirectly confirmed the relatively strong neutralizing capacities of the two

identified serum NAbs.

4. Discussion

In this study, we report that the combination of label-free FO-BLI technique with an effective signal enhancer DAB may facilitate the development of rapid biosensors for the sensitive detection of NAbs and BAbs. The sandwich FO-BLI BAbs biosensors have a sample-to-result time of 13 min. The competitive NAbs biosensor has a sample-to-result time of 7.5 min, making it even faster than the testing-on-a-probe biosensor, which is the fastest bioassay reported to date for surrogate NAbs assessment and has a result time of 18 min (Yang et al., 2021). Results obtained in such a short period provide important information to researchers or doctors regarding potent therapeutic NAbs agents or vaccine efficacies. BAbs and NAbs were measured individually in this study at their own speed; however, they can be well integrated for parallel detection by simply prolonging the 30 s of target detection

period of the NAb biosensor to 5 min (Table 1) to synchronize the speeds. Importantly, the easy-to-use dip-in sensors greatly simplify the assay operation and facilitate the routine use of these assays in laboratories, specifically for NAb detection, which typically requires strict BSL-3 laboratory environments.

The developed FO-BLI biosensors seem robust, as no additional blocking agents or blocking steps were needed to prevent possible non-specific binding from sera. Compared to the control of non-specific binding, precise control of desirable specific-binding is more delicate as DAB can significantly enhance the signals in seconds, which may result in lesser reproducibility between assays. For this purpose, the maximal shift intensities were controlled at approximately 15 nm when quantifying BAbS and NAbS in buffer and sera. Of note, a 200 × dilution of DAB enhancer was adopted throughout this work to avoid overloaded signals and to enhance the chance of regenerating sensors, as high amounts of precipitated DAB on the sensor tips can be challenging to remove. This study used a single sensor for one measurement; however, recycling sensors to reduce costs without compromising assay accuracy and speed, can be of interest for population-scale COVID-19 studies for high-throughput analysis (Goode et al., 2015).

Pre-clinical validation demonstrated that the FO-BLI NAbS biosensor could evaluate the inhibition of SARS-CoV-2 antibodies and aptamers with similar accuracy as an ELISA kit. A total of 16 participants that received the inactivated vaccines were enrolled in this study to validate the utility of the developed biosensors for use in clinical settings, rather than to evaluate the vaccine efficacy, as all the samples were taken randomly and most importantly, in limited numbers. Among the 16 participants, 14 were identified as anti-RBD antibody-positive (87.5%) using the anti-RBD BAb biosensor, which closely aligned with the data provided by the RBD antibody titer assay, with only a disagreement on one weak positive sample V-HD3. The anti-S-ECD BAb biosensor identified 14 participants (87.5%) as anti-S-ECD antibody positive, while only 6 (37.5%) were identified as NAb positive using the NAb biosensor. Overall, host humoral responses to vaccines differ significantly from person to person, as reflected by the antibody level diversity. The overall low levels of NAbS detected in all donors may be due to the less appropriate design of our sampling, as all random samples were collected rather late after injection (72 days [STD: 48.2] for the 14 second-dose sampled sera). In a recent phase 1/2 trial conducted by Xia et al. (2021), the production of NAbS in 100% of recipients was reported on day 28 post-injection of the second dose of BBIBP-CorV inactivated vaccine. Thus, evaluation of NAbS at earlier time points may reveal higher NAb rates and higher NAb concentrations or titers. Nevertheless, V-HD9 produced high-quality antibodies over time, with excellent binding and neutralizing activities toward RBD and pseudovirus. Such potent NAbS can be further isolated and engineered to evaluate their potential therapeutic outcomes (Guo et al., 2021). Interestingly, this small-cohort study reported the existence of NAbS in one sample collected approximately 6 months post-injection (V-HD15), indicating the long durability of NAb.

Future efforts should focus on the following aspects. First, the aforementioned approach is flexible and can be easily adapted to establish rapid biosensors for SARS-CoV-2 IgA, IgM, anti-S1, and anti-S2 in order to obtain a detailed profile of antibody response. In addition, it has the potential to be applied in sandwich-based SARS-CoV-2 antigen detection. Second, the rapid biosensors are suitable for continuous evaluation of humoral responses post vaccination or during infection, particularly owing to the readily available sample sources such as dried blood spots (Morley et al., 2020; Mulchandani et al., 2021; Bian et al., 2020) and saliva (Elledge et al., 2021). Third, a recent study revealed that it is more antibody affinity than antibody concentration that truly determines the inhibitory activity of an antibody in RBD-hACE2 binding (Fiedler et al., 2021). As thus, it would be of great value to upgrade the biosensors for direct use in undiluted whole blood or sera, as over-dilution affects the interaction of antibodies with the viral RBD. Of note, the nature of the BLI technique in real-time displaying molecule-molecule interactions

increases the possibility of developing our FO-BLI biosensors into a suitable system for determining antibody affinity and concentrations simultaneously. Finally, large-scale serosurveillance is encouraged to determine statistical rates for false positive and false negative results obtained using the established biosensors, in order to obtain better insights into the potency of vaccines (Zhang et al., 2021).

5. Conclusions

We report signal-enhanced FO-BLI biosensors for rapid detection of SARS-CoV-2 NAbS and BAbS in sera of vaccine-injected healthy donors. SARS-CoV-2 NAbS and BAbS could be measured either individually (7.5 min vs. 13 min, respectively) or simultaneously with only a one-step modification. The bioassays were clinically validated using a small cohort of randomly collected samples from 16 inactivated vaccines-injected healthy individuals. A detailed protocol was developed to detect BAbS against the RBD-N501Y variant, which helps to study the efficacy of new vaccines and therapeutic antibodies against coronavirus mutants. The advantages of the proposed FO-BLI biosensors lie in their capability of delivering a quick sample result, detecting with high sensitivity, operating in an automated manner, and monitoring NAbS and BAbS from real clinical samples with sufficient accuracy. Limitation of the study lies in its small number of real samples for systematic validation of the developed biosensors. In the following studies, we plan to enlarge the sample size and incorporate samples of infected persons for extra validation and evaluation of the clinical utility of biosensors. Also, we plan to explore the potentials of the FO-BLI biosensors for long-term evaluation of dynamic humoral responses, for simultaneous detection of antibody concentration and affinity, and for detection in alternative sample matrices.

CRedit authorship contribution statement

Sumin Bian: Conceptualization, Methodology, Experiments, Analysis, Writing, Reviewing, Editing. Min Shang: Recruiting volunteers, Collection of serum samples, Reviewing. Mohamad Sawan: Supervision, Reviewing, Funding acquisition.

Declaration of competing interest

The authors declare that they have no known competing financial interests or personal relationships that could have appeared to influence the work reported in this paper.

Acknowledgements

We thank all the study volunteers for contributing their blood samples. We are grateful for funding support from the Westlake University [Grant No. 10318A992001]; Tencent Foundation [Grant No. XHTX202003001]; Research Program on COVID-19 of Zhejiang University of Technology; the Leading Innovative and Entrepreneur Team Introduction Program of Zhejiang [Grant No. 2020R01005]; and National Natural Science Foundation of China [Grant No. 82104122].

References

- Ali, M.A., Hu, C., Jahan, S., Yuan, B., Saleh, M.S., Ju, E., Gao, S.J., Panat, R., 2021. *Adv. Mater.* 33, 2006647.
- Auer, S., Koho, T., Uusi-Kerttula, H., Vesikari, T., Blazevic, V., Hyytönen, V.P., 2015. *Sensor. Actuator. B Chem.* 221, 507–514.
- Bian, S., Ferrante, M., Gils, A., 2017. *AAPS J.* 19, 468–474.
- Bian, S., Lu, J., Delpont, F., Vermeire, S., Spasic, D., Lammertyn, J., Gils, A., 2018. *Drug Test. Anal.* 10 (3), 592–596.
- Bian, S., Stappen, T.V., Baert, F., Compennolle, G., Brouwers, E., Tops, S., de Vries, A., Rispens, T., Lammertyn, J., Vermeire, S., Gils, A., 2016. *J. Pharm. Biomed. Anal.* 125, 62–67.
- Bian, S., Van den Berghe, N., Vandersmissen, L., Tops, S., Vermeire, S., Ferrante, M., Gils, A., Thomas, D., 2020. *J. Pharm. Biomed. Anal.* 185, 113224.

- Dzimianski, J.V., Lorig-Roach, N., O'Rourke, S.M., Alexander, D.L., Kimmey, J.M., DuBois, R.M., 2020. *Sci. Rep.* 10 (1), 21738.
- Elledge, S.K., Zhou, X.X., Byrnes, J.R., Martinko, A.J., Lui, I., Pance, K., Lim, S.A., Glasgow, J.E., Glasgow, A.A., Turcios, K., Iyer, N., Torres, L., Peluso, M.J., Henrich, T.J., Wang, T.T., Tato, C.M., Leung, K.K., Greenhouse, B., Wells, J.A., 2021. *Nat. Biotechnol.* 39 (8), 928–935.
- Fiedler, S., Piziorska, M.A., Denninger, V., Morgunov, A.S., Ilsley, A., Malik, A.Y., Schneider, M.M., Devenish, S.R.A., Meisl, G., Kosmoliaptis, V., Aguzzi, A., Fiegler, H., Knowles, T.P.J., 2021. *ACS Infect. Dis.* acsinfedcis.1c00047.
- Funari, R., Chu, K.Y., Shen, A.Q., 2020. *Biosens. Bioelectron.* 169, 112578.
- Gandolfini, I., Harris, C., Abecassis, M., Anderson, L., Bestard, O., Comai, G., Cravedi, P., Cremaschi, E., Duty, J.A., Florman, S., Friedewald, J., La Manna, G., Maggiorem, U., Moran, T., Piotti, G., Purroy, C., Jarque, M., Nair, V., Shapiro, R., Reid-Adam, J., Heeger, P.S., 2017. *Kidney Int. Rep.* 2 (6), 1186–1193.
- Gao, S.X., Zheng, X., Hu, B., Sun, M.J., Wu, J.H., Jiao, B.H., Wang, L.H., 2017. *Biosens. Bioelectron.* 89, 952–958.
- Goode, J.A., Rushworth, J.V., Millner, P.A., 2015. *Langmuir* 31 (23), 6267–6276.
- Guo, Y., Huang, L., Zhang, G., Yao, Y., Zhou, H., Shen, S., Shen, B., Li, B., Li, X., Zhang, Q., Chen, M., Chen, D., Wu, J., Fu, D., Zeng, X., Feng, M., Pi, C., Wang, Y., Zhou, X., Lu, M., Li, Y., Fang, Y., Lu, Y.Y., Hu, X., Wang, S., Zhang, W., Gao, G., Adrian, F., Wang, Q., Yu, F., Peng, Y., Gabibov, A.G., Min, J., Wang, Y., Huang, H., Stepanov, A., Zhang, W., Cai, Y., Liu, J., Yuan, Z., Zhang, C., Lou, Z., Deng, F., Zhang, H., Shan, C., Schweizer, L., Sun, K., Rao, Z., 2021. *Nat. Commun.* 12 (1), 2623.
- He, Z., Ren, L., Yang, J., Guo, L., Feng, L., Ma, C., Wang, X., Leng, Z., Tong, X., Zhou, W., Wang, G., Zhang, T., Guo, Y., Wu, C., Wang, Q., Liu, M., Wang, C., Jia, M., Hu, X., Wang, Y., Zhang, X., Hu, R., Zhong, J., Yang, J., Dai, J., Chen, L., Zhou, X., Wang, J., Yang, W., Wang, C., 2021. *Lancet* 397 (10279), 1075–1084.
- Huo, J., Le Bas, A., Ruza, R.R., Duyvesteyn, H.M.E., Mikolajek, H., Malinauskas, T., Tan, T.K., Rijal, P., Dumoux, M., Ward, P.N., Ren, J., Zhou, D., Harrison, P.J., Weckener, M., Clare, D.K., Vogirala, V.K., Radecke, J., Moynié, L., Zhao, Y., Gilbert-Jaramillo, J., Knight, M.L., Tree, J.A., Buttigieg, K.R., Coombes, N., Elmore, M.J., Carroll, M.W., Carrique, L., Shah, P.N.M., James, W., Townsend, A.R., Stuart, D.I., Owens, R.J., Naismith, J.H., 2020. *Nat. Struct. Mol. Biol.* 27 (9), 846–854.
- Krammer, F., Srivastava, K., 2021. The PARIS Team. Simon, V. medRxiv. 2021.01.29.21250653.
- Legros, V., Denolly, S., Vogrig, M., Bosen, B., Siret, E., Rigaiil, J., Pillet, S., Grattard, F., Gonzalo, S., Verhoeven, P., Allatif, O., Berthelot, P., Pélissier, C., Thiery, G., Botelho-Nevers, E., Millet, G., Morel, J., Paul, S., Walzer, T., Cosset, F.L., Bourlet, T., Pozzetto, B., 2021. *Cell. Mol. Immunol.* 18, 318–327.
- Liu, G.Q., Rusling, J.F., 2021. *ACS Sens.* 6 (3), 593–612.
- Lu, J.D., Van Stappen, T., Spasic, D., Delpoit, F., Vermeire, S., Gils, A., Lammertyn, J., 2016. *Biosens. Bioelectron.* 79, 173–179.
- Morley, G.L., Taylor, S., Jossi, S., Perez-Toledo, M., Faustini, S.E., Marcial-Juarez, E., Shields, A.M., Goodall, M., Allen, J.D., Watanabe, Y., Newby, M.L., Crispin, M., Drayson, M.T., Cunningham, A.F., Richter, A.G., O'Shea, M.K., 2020. *Emerg. Infect. Dis.* 26 (12), 2970–2973.
- Mulchandani, R., Brown, B., Brooks, T., Semper, A., Machin, N., Linley, E., Borrow, R., Wyllie, D., EDSAB-HOME Study Investigators, 2021. *J. Clin. Virol.* 136, 104739.
- Nie, J., Li, Q., Wu, J., Zhao, C., Hao, H., Liu, H., Zhang, L., Nie, L., Qin, H., Wang, M., Lu, Q., Li, X., Sun, Q., Liu, J., Fan, C., Huang, W., Xu, M., Wang, Y., 2020. *Emerg. Microb. Infect.* 1, 680–686.
- Papamichael, K., Cheifetz, A.S., Melmed, G.Y., Irving, P.M., Vande Castele, N., Kozuch, P.L., Raffals, L.E., Baidoo, L., Bressler, B., Devlin, S.M., Jones, J., Kaplan, G. G., Sparrow, M.P., Velayos, F.S., Ullman, T., Siegel, C.A., 2019. *Clin. Gastroenterol. Hepatol.* 17 (9), 1655–1668 e3.
- Song, Y., Song, J., Wei, X., Huang, M., Sun, M., Zhu, L., Lin, B., Shen, H., Zhu, Z., Yang, C., 2020. *Anal. Chem.* 92 (14), 9895–9900.
- Stringhini, S., Wisniak, A., Piumatti, G., Azman, A.S., Lauer, S.A., Baysson, H., De Ridder, D., Petrovic, D., Schrepff, S., Marcus, K., Yerly, S., Arm Vernez, I., Keiser, O., Hurst, S., Posfay-Barbe, K.M., Trono, D., Pittet, D., Gétaz, L., Chappuis, F., Eckler, I., Vuilleumier, N., Meyer, B., Flahault, A., Kaiser, L., Guessous, I., 2021. *Lancet* 396 (10247), 313–319.
- Swank, Z., Michielin, G., Yip, H.M., Cohen, P., Andrey, D.O., Vuilleumier, N., Kaiser, L., Eckler, I., Meyer, B., Maerkl, S.J., 2021. *Proc. Natl. Acad. Sci. U. S. A.* 118 (18), e2025289118.
- Tan, C.W., Chia, W.N., Qin, X., Liu, P., Chen, M.I., Tiu, C., Hu, Z., Chen, V.C., Young, B.E., Sia, W.R., Tan, Y.J., Foo, R., Yi, Y., Lye, D.C., Anderson, D.E., Wang, L.F., 2020. *Nat. Biotechnol.* 38 (9), 1073–1078.
- Tan, X., Krel, M., Dolgov, E., Park, S., Li, X., Wu, W., Sun, Y.L., Zhang, J., Khaing, Oo M. K., Perlin, D.S., Fan, X., 2020. *Biosens. Bioelectron.* 169, 112572.
- Torrente-Rodríguez, R.M., Lukas, H., Tu, J., Min, J., Yang, Y., Xu, C., Rossiter, H.B., Gao, W., 2020. *Matter* 3 (6), 1981–1998.
- Wajnberg, A., Amanat, F., Firpo, A., Altman, D.R., Bailey, M.J., Mansour, M., McMahon, M., Meade, P., Mendu, D.R., Muellers, K., Stadlbauer, D., Stone, K., Strohmeier, S., Simon, V., Aberg, J., Reich, D.L., Krammer, F., Cordon-Cardo, C., 2020. *Science* 370 (6521), 1227–1230.
- Xia, S., Zhang, Y., Wang, Y., Wang, H., Yang, Y., Gao, G.F., Tan, W., Wu, G., Xu, M., Lou, Z., Huang, W., Xu, W., Huang, B., Wang, H., Wang, W., Zhang, W., Li, N., Xie, Z., Ding, L., You, W., Zhao, Y., Yang, X., Liu, Y., Wang, Q., Huang, L., Yang, Y., Xu, G., Luo, B., Wang, W., Liu, P., Guo, W., Yang, X., 2021. *Lancet Infect. Dis.* 21 (1), 39–51.
- Yang, H.S., Racine-Brzostek, S.E., Karbaschi, M., Yee, J., Dillard, A., Steel, P.A.D., Lee, W. T., McDonough, K.A., Qiu, Y., Ketas, T.J., Francomano, E., Klasse, P.J., Hatem, L., Westblade, L., Wu, H., Chen, H., Zuk, R., Tan, H., Girardin, R.C., Dupuis, A.P. 2nd, Payne, A.F., Moore, J.P., Cushing, M.M., Chadburn, A., Zhao, Z., 2021. *Biosens. Bioelectron.* 178, 113008.
- Zhang, Y., Zeng, G., Pan, H., Li, C., Hu, Y., Chu, K., Han, W., Chen, Z., Tang, R., Yin, W., Chen, X., Hu, Y., Liu, X., Jiang, C., Li, J., Yang, M., Song, Y., Wang, X., Gao, Q., Zhu, F., 2021. *Lancet Infect. Dis.* 21 (2), 181–192.
- Zhou, B., Thao, T.T.N., Hoffmann, D., Taddeo, A., Ebert, N., Labrousseau, F., Pohlmann, A., King, J., Steiner, S., Kelly, J.N., Portmann, J., Halwe, N.J., Ulrich, L., Trüeb, B.S., Fan, X., Hoffmann, B., Wang, L., Thomann, L., Lin, X., Stalder, H., Pozzi, B., de Brot, S., Jiang, N., Cui, D., Hossain, J., Wilson, M.M., Keller, M.W., Stark, T.J., Barnes, J.R., Dijkman, R., Jores, J., Benarafa, C., Wentworth, D.E., Thiel, V., Beer, M., 2021. *Nature* 592, 122–127.
- Zhou, G., Zhao, Q., 2020. *Int. J. Biol. Sci.* 16 (10), 1718–1723.